


STUDY OF CRACK ORIENTATION OF UNDISTURBED MILE EXPANSIVE SOIL VIA X-RAY COMPUTED TOMOGRAPHY

Waseda University, Student Member,  Danxi Sun
Southwest Jiaotong University, Guanlu Jiang Xianfeng Liu
Waseda University, Member, Komine Hideo Hailong Wang

1. INTRODUCTION

The effect of the crack in the soil is not a trivial matter. The desiccation crack in soil not only affects the strength of soil, but also provides convenient channels for infiltration and evaporation (Rayhani *et al.*, 2007). The influence of water aggravates the soil expansion and shrinkage, especially in the expansive soil. In recent years, the use of computer for seepage simulation is becoming more and more popular. It is important to get the distribution and shape features of cracks during the process of establishing a three-dimensional crack network model for seepage simulation. In terms of the orientation of crack, a computerized method for analyzing clusters of orientation data was developed and the orientation of crack obeys normal distribution and has a mean value in the prevailing orientation (Mahtab, 1972). This has also been proved in excavation-induced cracks of clay (Huysmans *et al.*, 2006). In conclusion, most scholars (Einstein *et al.*, 1978; Priest, 1980; Wallis and King, 1980; Li and Zhang, 2010) conclude that the crack orientation is normally distributed, while a few scholars (Baecher *et al.*, 1977) believe that it is uniformly distributed. However, few scholars study the change of orientation during the development of cracks in undisturbed soil. Therefore, the research on the variation of crack orientation during drying is of great significance to the simulation of seepage flow.

In order to study the evolution of crack orientation (represented by the crack angle (θ_h) in this study) in specimens, CT scans and quantitative analysis of undisturbed expansive soil were carried out via Avizo software. Based on these, θ_h of soil specimens were calculated and summarized. Finally, the distribution of θ_h was fitted by the normal integral function and the development process of θ_h during drying was described by the fitting parameter σ .

2. MATERIALS, EQUIPMENTS AND PROCEDURES

The sampling spot is located in Mile basin, Yunnan, China and close to the KunMing-NanNing high-speed railway (referred to as "KNHR"). Some undisturbed soil specimens (about 200mm in height and 100mm in diameter) were also retrieved from the site using the tube sampling method according to the Chinese field-testing standard (JGJ/T87-2012). Fundamental soil properties can be seen in Table 1.

Four specimens with different suction values were selected for this study and the basic information can be seen in table 2. Among them, No.1, No.2, and No.3 were sealing by iron sheets and plastic films immediately after retrieving. However, No.4 was dried in the air and then sealed for equilibrium. Two weeks later, suction values of specimens were measured by WP4C Water Potential Meter and High-capacity Tensiometer. The measuring range of WP4C is 0~300MPa. When the measured value is in the range of 0~5MPa, the error of WP4C is ± 0.05 MPa. And the error will be 1% if the measured value is in the range of -5MPa~300MPa. For High-capacity Tensiometer, the measuring range and the error are 0~1.5MPa and 0.1kpa respectively. It worth noting that all soil specimens were taken from the depth of 0-4m from the ground. Thus, WP4C were used to measure soil specimens with suction greater than 1 MPa. In contrast, High-capacity Tensiometer were used when the suction of the specimen is lower than 1 MPa.

Emotion 16 CT machine from Siemens was used in this study. Finally, a series of original CT images containing 512×512 pixels with a layer thickness of 6 mm were obtained. Based on these images, three-dimensional reconstruction (see Fig. 1) and skeletonization (see Fig. 2) of cracks of four specimens obtained via a series of the process including median filter, interactive thresholding, opening, closing, erosion, and skeleton. It is worth noting that two nodes and a series of points form a Segment and the definition of θ_h can be seen in Fig 2.

3. RESULTS AND DISCUSSION

Stratigraphic angles (see Fig. 3 (a)) were obtained from the statistics of the geological prospecting data of KunMing-NanNing high-speed railway near the sampling site. The

Table 1 Fundamental soil properties of Mile expansive soils

Depth (m)	Minerology composite by XRD analysis				CEC (meq/100g)	G_s
	Montmorillonite (%)	Illite (%)	Kaolinite (%)	Chlorite (%)		
0.3-0.5	/	/	/	/	/	2.77
2.4-2.6	22.41	16.5	21.1	13.2	31.3	2.78
3.3-3.5	27.67	/	/	/	36.5	/

Note: CEC means cation exchange capacity. G_s means relative density of particle

Table 2 Summary of basic information of specimens

Number	Suction (MPa)	Water content (%)	Process
1	0.56	18.6	sealing
2	1.7	20.3	sealing
3	4.63	19.9	sealing
4	6.45	14.6	sealing after drying

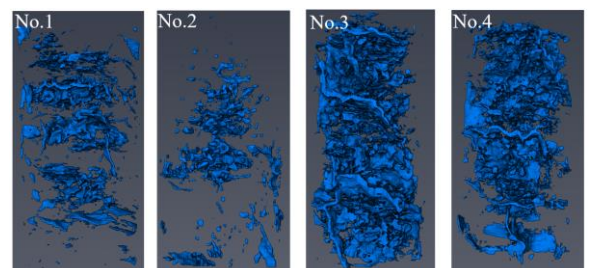


Fig. 1 Three-dimensional reconstruction of cracks

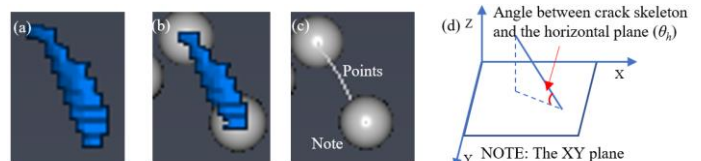


Fig. 2 Process of skeleton (a) One segment of cracks (b) Skeletonization of the fragment (c) Removal of crack (d) Definition of θ_h

Keywords: Undisturbed expansive Soil, CT Scan, Crack Behavior, Crack Orientation

Contact Address: sundanxililin@ruri.waseda.jp, 3-4-1, Okubo, Shinjyuku-ku, Tokyo 169-8555, Japan, Tel: +81-(0)3-5286-2940

stratigraphic angles are the angle between the horizontal plane and the interface of different soils. From Fig. 3(a), we can see that angle distribution curves intersect between $20^\circ \sim 30^\circ$ and $30^\circ \sim 40^\circ$. The angle ratio is reversed before and after the intersection point. This means that compared with the high-suction soil specimens, the low-suction soil specimens have higher small-angle ratios, while the high-suction specimens have higher large-angle ratios. Therefore, there are more large-angle cracks in the newly developed cracks during drying. In stratigraphic angle statistics, all stratigraphic angles are between 0° and 30° , indicating that the primary-cracks already existed or the primary-cracks ready to be opened are within this range of angle. The distribution of θ_h was fitted by the normal integral function as follow:

$$\theta_r = 2 \times \int_{\alpha}^{\alpha+1} \frac{1}{\sqrt{2\pi}\sigma} e^{-\frac{x^2}{2\sigma^2}} dx \quad (1)$$

Where θ_h is the ratio of crack segments within a certain range of angles; α corresponds to the angular range; σ is the fitting parameter.

It is worth noting that the integral range here is $(\alpha, \alpha+1)$ corresponding to the angle range. The fitting results can be seen from Fig. 3(c) to Fig. 3(f), and the results of the fitting parameter (σ) were summarized in Fig. 3(b). As the suction increases, the increment of σ decreases gradually.

The crack in undisturbed expansive soil development pattern showed in Fig. 4. No crack develops in the initial state (Fig. 4 (a)). During the drying process, the soil shrinks gradually, and primary cracks begin to develop in the soil layer where is the structural weakness of soil (see Fig.4 (b)). After the primary cracks initiating, the sub-cracks initiate at existing primary cracks and almost perpendicular to the primary cracks due to the drying and shrinkage process of the surface of the primary cracks (see Fig.4 (c)). Of course, the primary cracks may exist in the initial state. Thus, the crack development may begin from Fig.4 (b). It worth noting that the schematic diagram does not indicate that the primary crack does not develop as the suction increases.

4. CONCLUSIONS

Crack orientation in undisturbed expansive soil follows normal distribution. This phenomenon has a great correlation with the soil layer angles and can be explained from the aspect of cracking mechanism. Based on these, θ_h is fitted by the normal integral function and a series of σ were obtained. Subsequently, the relationship between σ and suctions is discussed in this paper: σ increases as the suction increases and the trend of growth is slowing down in high suction range.

REFERENCES:

- Baecher, G. B., Lanney, N. A. and Einstein, H. H. (1977) 'Statistical description of rock properties and sampling', in *The 18th US Symposium on Rock Mechanics (USRMS)*. American Rock Mechanics Association.
- Einstein, H. H. et al. (1978) 'Decision analysis applied to rock tunnel exploration', *Engineering Geology*, 12, pp. 143–161.
- Huysmans, M., Berckmans, A. and Dassargues, A. (2006) 'Effect of excavation induced fractures on radionuclide migration through the Boom Clay (Belgium)', *Applied clay science*, 33(3–4), pp. 207–218.
- Li, J. H. and Zhang, L. M. (2010) 'Geometric parameters and REV of a crack network in soil', *Computers and Geotechnics*, 37(4), pp. 466–475.
- Mahtab, M. A. (1972) *Analysis of fracture orientations for input to structural models of discontinuous rock*. US Department of Interior, Bureau of Mines.
- Priest, S. D. (1980) 'The use of inclined hemisphere projection methods for the determination of kinematic feasibility, slide direction and volume of rock blocks', in *International Journal of Rock Mechanics and Mining Sciences & Geomechanics Abstracts*. Elsevier, pp. 1–23.
- Rayhani, M. H. T., Yanful, E. K. and Fakher, A. (2007) 'Desiccation-induced cracking and its effect on the hydraulic conductivity of clayey soils from Iran', *Canadian geotechnical journal*, 44(3), pp. 276–283.
- Wallis, R. F. and King, M. S. (1980) 'Discontinuity spacings in a crystalline rock', in *International Journal of Rock Mechanics and Mining Sciences & Geomechanics Abstracts*. Elsevier, pp. 63–66.

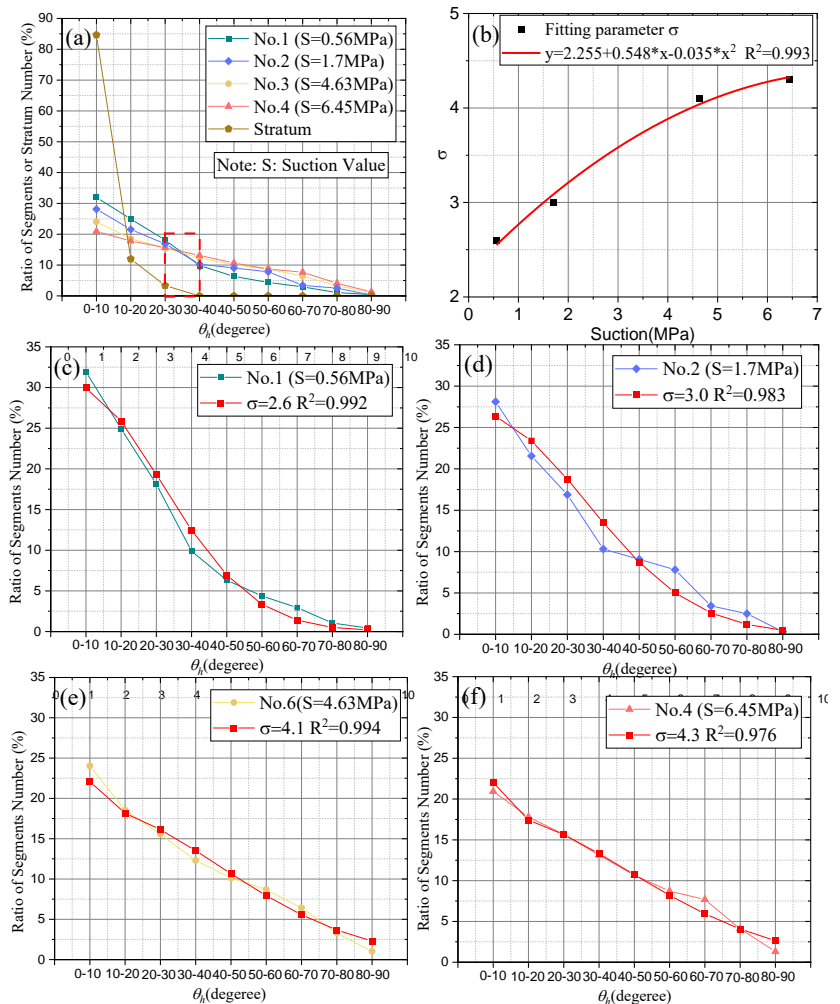


Fig. 3 Comparison of angle ratios with different suctions and fitting curves

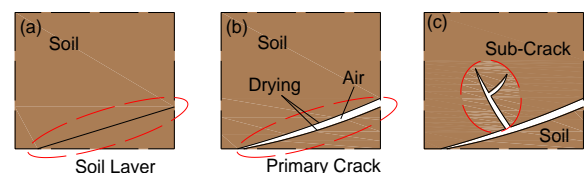


Fig. 4 The evolution of primary cracks and sub-cracks in situ

Of course, the primary cracks may exist in the initial state. Thus, the crack development may begin from Fig.4 (b). It worth noting that the schematic diagram does not indicate that the primary crack does not develop as the suction increases.